Electronic supplementary information (ESI)

An investigation on PANI/NENP-1 composite as a novel photocatalyst for photocatalytic dye wastewater degradation

Heling Zhang[a], Huaizhi Yang[a], Qingrong Cheng[a], Zhiquan Pan[a]

[a] School of Chemistry and Environmental Engineering, Wuhan Institute of Technology, Wuhan, 430205, PR China.

Corresponding authors:

*(Q.C.) E-mail: chengqr383121@sina.com

Total number of pages: 6

Total number of Tables: 1

Total number of Figures: 6

Characterization

The powder X-ray diffraction (PXRD) pattern was recorded on the Bruker D8 Advance X-ray diffractometer (Cu Kα, λ = 1.54056 nm), in the range between 10°and 80° with a scanning rate of 5° min^{-1} at 40 kV accelerating voltage and 40 mA current. Fourier transformed infrared spectroscopy (FT-IR) in the wavelength range of 4000 ~ 400 cm^{-1} (KBr tablet) was performed by Nicolet 6700 spectrometer. The morphology and structure of PANI monomer, NENP-1 and $PANI_5$/NENP-1 were observed with a scanning electron microscope (Zeiss GeminiSEM 300) under the acceleration voltage of 15 kV. The transmission electron microscope (TEM) images were measured using JEOL JEM-2100F microscope at 200 kV. X-ray photoelectron spectroscopy (XPS) measurements were performed on a Themo Fisher ESCALAB XI+ spectrometer and using Mg Kα radiation as the nonmonochromatized source (hν=1253.6eV). The electronic binding energy (BE) of the elements was corrected based on C1s (284.6 eV). Thermogravimetric analysis (TGA) of the material measured on an Netzsh STA 449F3 instrument in the temperature range of 30–800 °C and the heating rate of 10 °C min^{-1} under a nitrogen atmosphere. Optical properties were analyzed by using UV–vis diffuse reflectance spectra (DRS, Shimadzu UV 2600) and wavelengths ranging from 200 nm to 800 nm. The photoelectrochemical properties of all prepared materials were tested using a CHI 660E electrochemical workstation (Chenhua Company). The Mott-Schottky (MS) plots were collected by conducting impedance-potential spectroscopy at 10 kHz in 0.5 M Na_2SO_4 solution versus silver chloride electrode (Ag/AgCl). The electron spin resonance (ESR) spectrum was measured by using a Bruker EPR A 300-10/12 spectrometer to tracing the activated species.

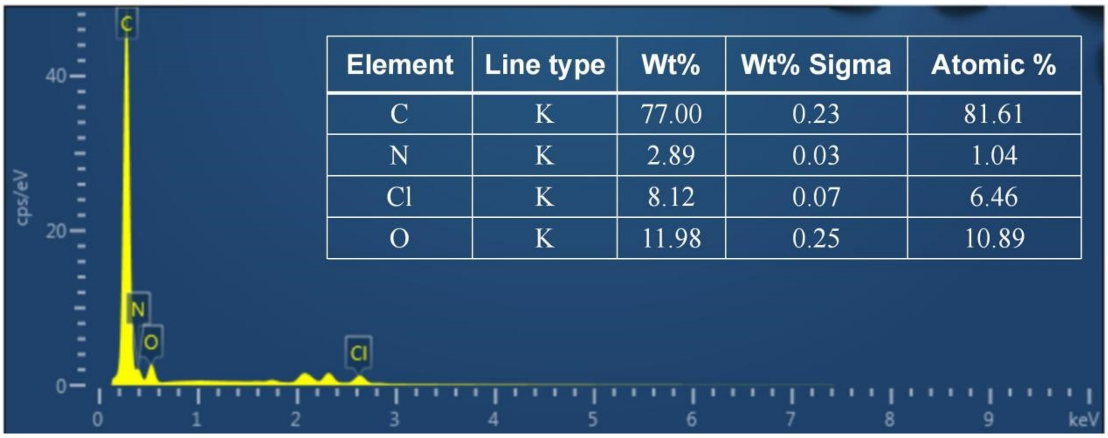

Element	Line type	Wt%	Wt% Sigma	Atomic %
C	K	77.00	0.23	81.61
N	K	2.89	0.03	1.04
Cl	K	8.12	0.07	6.46
O	K	11.98	0.25	10.89

Figure S1 The EDS pattern of $PANI_5$/NENP-1.

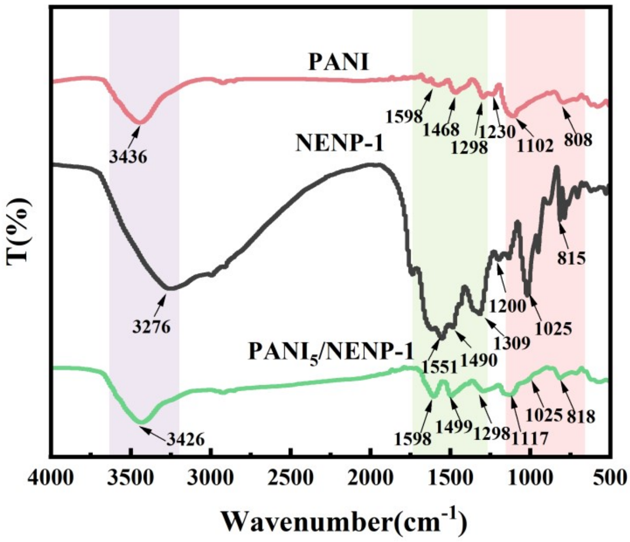

Figure S2 FT-IR spectra of PANI、NENP-1 and $PANI_5$/NENP-1.

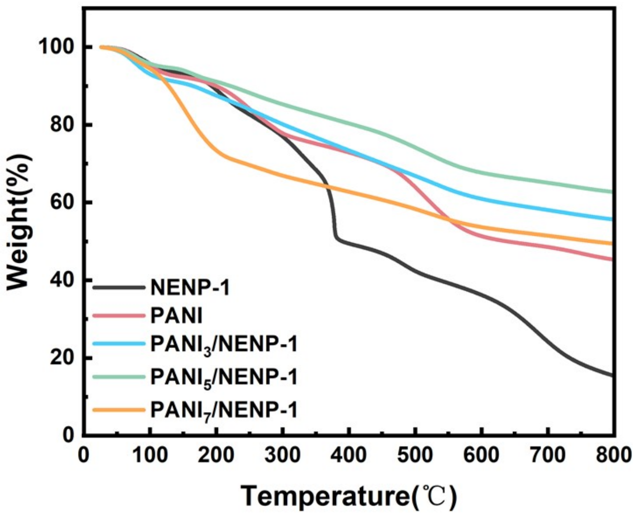

Figure S3 TG curves of all prepared materials.

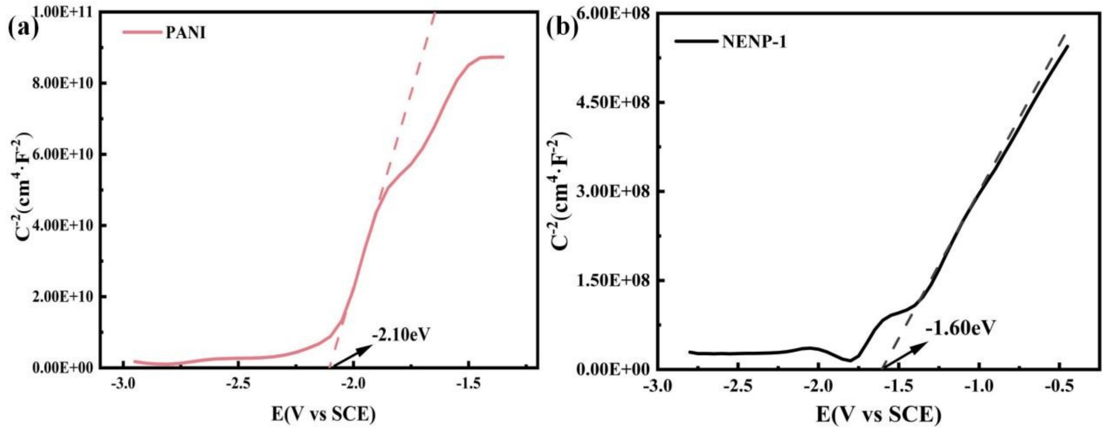

Figure S4 Mott-Schottky plots for (a) PANI and (b) NENP-1.

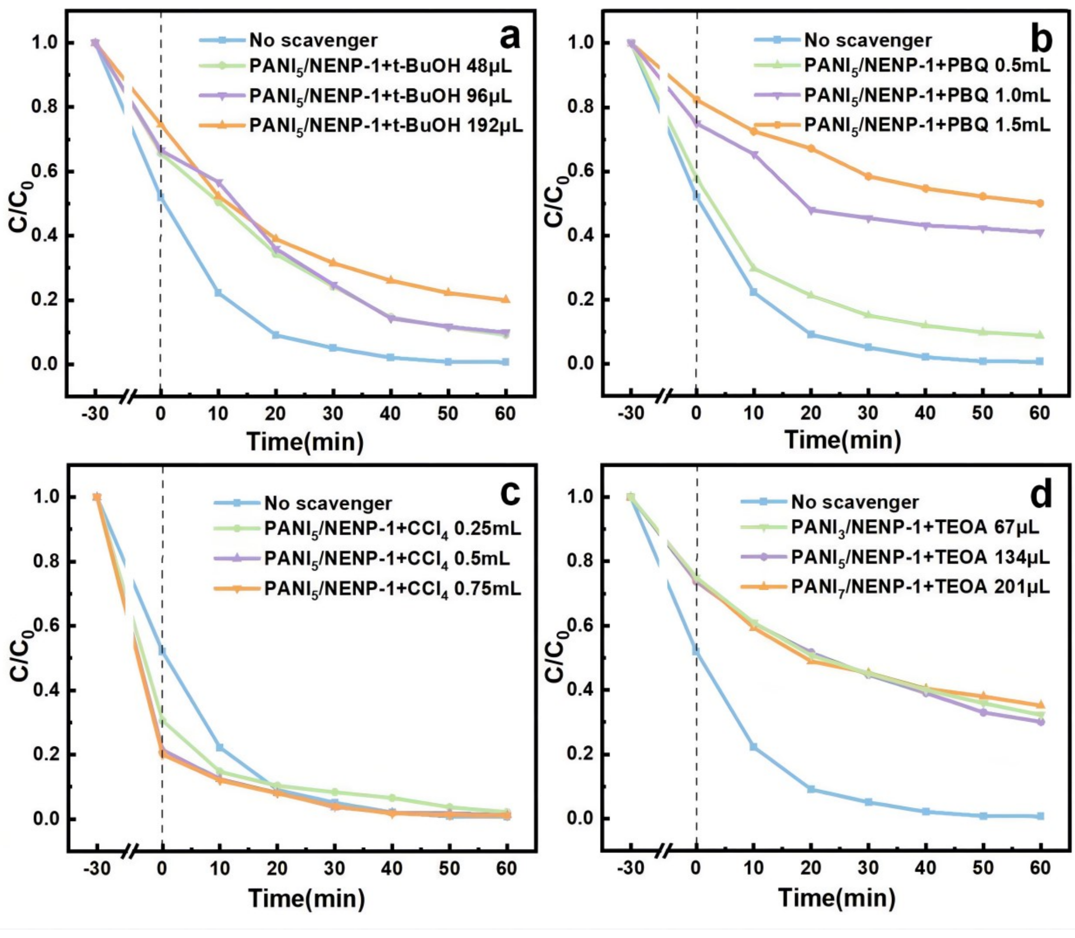

Figure S5 (a-d) The radical trapping test of photocatalysts with different dosages.

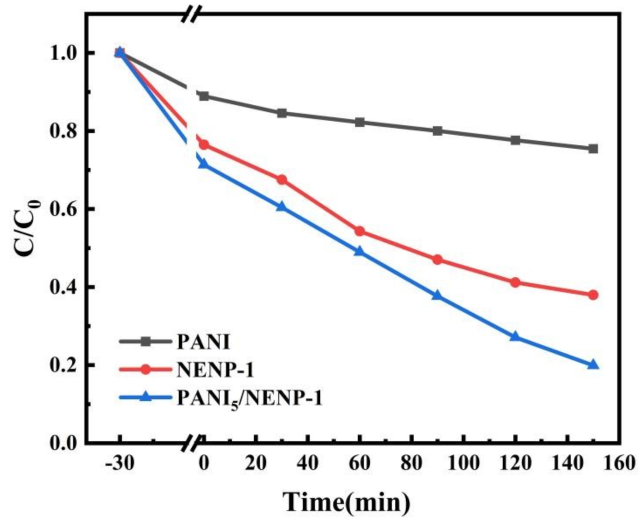

Figure S6 Photocatalytic degradation of 2-chlorophenol over PANI, NENP-1, and and $PANI_5$/NENP-1under sunlight irradiation.

Catalyst/mg	Dye	V(mL)/C_0 (mg·L^{-1})	Light source (λ>420nm)	Time (min)	Result (%)	TOF	Ref.
PANI/NENP-1/10	RhB	50/20	Sun light	60	100	0.00167	This work
PANI/NENP-1/10	MO	50/20	Sun light	60	100	0.00167	This work
MoO_3/MoS_2/10	RhB	50/10	Sun light	120	80~90	0.000416	[1]
MoS_2/BiOI/10	RhB	50/5	Visible light	90	100	0.000277	[2]
Bi_2WO_6 QDS/g-C_3N_4/50	RhB	50/10	Sun light	30	100	0.000333	[3]
PANI/CdS/100	RhB	200/5	Visible light	60	100	0.000167	[4]
Bi_2WO_6/50	RhB	100/5	Visible light	60	99.5	0.000167	[5]
Co_3O_4/TiO_2/100	MO	50/100	Visible light	120	88	0.000367	[6]
$AgBr/Ag_3PO_4$/100	MO	50/10	Visible light	50	100	0.0001	[7]

Table S1 Comparison of the RhB and MO degradation capacity of $PANI_5$/NENP-1 with other photocatalysts.

TOF is calculated according to an equation: $TOF = \frac{C_0 \times V_{RhB/MO} \times \text{Degradation rate}}{m_{\text{catalyst}} \times t}$

References

[1] Chen J, Liao Y, Wan X *et al.* A high performance MoO_3@MoS_2 porous nanorods for adsorption and photodegradation of dye. Journal of Solid State Chemistry 2020; 291.https://doi.org/10.1016/j.jssc.2020.121652.

[2] Hao L, Ju P, Zhang Y *et al.* Fabrication of hierarchical flower-like BiOI/MoS_2 heterostructures with highly enhanced visible-light photocatalytic activities. Colloids and Surfaces A: Physicochemical and Engineering Aspects 2021; 610.https://doi.org/10.1016/j.colsurfa.2020.125714.

[3] Chen W, Liu T-Y, Huang T *et al.* In situ fabrication of novel Z-scheme Bi_2WO_6 quantum dots/g-C_3N_4 ultrathin nanosheets heterostructures with improved photocatalytic activity. Applied Surface Science 2015; 355:379-387.https://doi.org/10.1016/j.apsusc.2015.07.111.

[4] Sharma S, Kumar D, Khare N. Hierarchical PANI/CdS nanoarchitecture system for visible light induced photocatalytic dye degradation and photoelectrochemical water splitting. Polymer 2021; 231.https://doi.org/10.1016/j.polymer.2021.124117.

[5] Fu H, Pan C, Yao W, Zhu Y. Visible-light-induced degradation of rhodamine B by nanosized Bi_2WO_6. J Phys Chem B 2005; 109:22432-22439.https://doi.org/10.1021/jp052995j.

[6] Saeed M, Usman M, Ibrahim M *et al.* Enhanced photo catalytic degradation of methyl orange using p–n Co_3O_4-TiO_2 hetero-junction as catalyst. International Journal of Chemical Reactor Engineering 2020; 18.https://doi.org/10.1515/ijcre-2020-0004.

[7] Cao J, Luo B, Lin H *et al.* Visible light photocatalytic activity enhancement and mechanism of AgBr/Ag_3PO_4 hybrids for degradation of methyl orange. J Hazard Mater 2012; 217-218:107-115.https://doi.org/10.1016/j.jhazmat.2012.03.002.